Quantum Chemical Study on Enantioselective Reduction of Aromatic Ketones Catalyzed by Chiral Cyclic Sulfur-Containing Oxazaborolidines. Part 3. Structures of Catalyst–Alkoxyborane Adducts

MING LI,* RUGANG XIE, XAIRONG HU, ANMIN TIAN
Department of Chemistry, Sichuan University, Chengdu 610064, People's Republic of China

Received 24 September 1999; accepted 21 December 1999

ABSTRACT: The chiral cyclic sulfur-containing oxazaborolidine catalyst reacts with aromatic ketone in the presence of borane to form the catalyst–alkoxyborane adduct with a B-O-B-N four-membered ring. The ab initio molecular orbital method is employed to study the structures of the catalyst–alkoxyborane adduct. All the calculated systems are optimized completely by means of the Hartree–Fock method at 6-31g* basis sets. The B-O-B-N four-membered ring is stable, although there is strong tensile stress in the four-membered ring. The catalyst–alkoxyborane adduct exists in four stable structures. Among these structures, the largest energy difference is only about 4 kJ/mol. In the catalyst–alkoxyborane adduct, the B(2)—N(3) bond in the catalyst is weakened greatly.

Key words: ab initio; cyclic sulfur-containing oxazaborolidine; enantioselective reduction; catalyst–alkoxyborane adduct

Correspondence to: A. Tian.
**Permanent address:* Department of Chemistry, Southwest-China Normal University, Chongqing 400715, People's Republic of China.
Contract grant sponsors: Science Foundation of the National Education Department; Science Foundation of Chongqing City, People's Republic of China.

Introduction

In recent years, the chiral cyclic sulfur-containing oxazaborolidine **1** has been synthesized by replacement of pyrrolidine with thiazolidine in the CBS catalysts **1a** and used, as a new type of effective catalyst in the enantioselective catalytic reduction of ketone [1–4]. As shown in the experiments [1–4], the chirality of the reduced products determined by the catalyst **1** is opposite to that determined by the CBS catalyst **1a**. In general, when the oxazaborolidine **1a**, which is of a S chirality at the C4 site, is used in the enantioselective reduction of aromatic ketone with borane, (R) alcohols are obtained. However, when the enantioselective reduction of aromatic ketone is catalyzed by the catalyst **1** arising from the (4S)-CBS catalyst **1a**, (S) alcohols are obtained. This is significant not only for synthetic chemistry, but also for theoretical chemistry. For the purpose of convenient discussion, the catalyst **1** is termed the Chengdu–Taipei–Oldenburg (CTO) catalyst in the article.

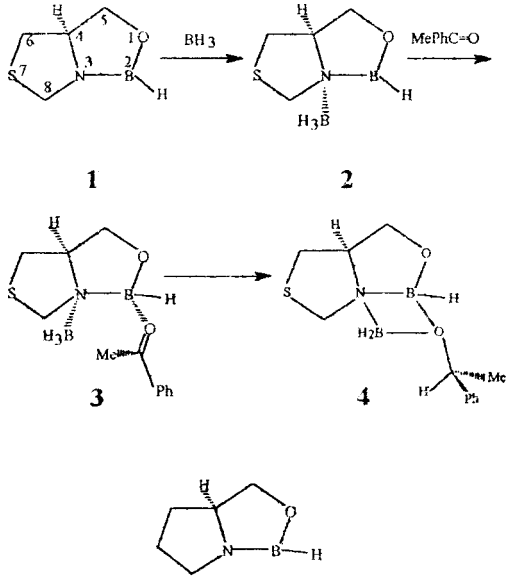

The mechanism of the enantioselective reduction of ketone catalyzed by the CBS catalyst was suggested by Corey et al. [5]. According to this mechanism of catalysis, the enantioselective reduction of aromatic ketone catalyzed by the CTO catalyst mainly involves the following steps: formation of the CTO–borane adduct **2**; coordination of aromatic ketone to be reduced to the adduct **2**, leading to the CTO–borane–ketone adduct **3**; hydride transfer from the borane moiety to the carbonyl carbon in the adduct **3** to form the CTO–alkoxyborane adduct **4**. The reduced products are the chiral alcohols $R_LR_SC(OH)H$. Quantum chemical modeling studies on the enantioselective reduction catalyzed by the oxazaborolidine **1a** (the CBS catalyst), in which the simplified molecular models were used, were carried out by Nevalainen [6–12] by means of the ab initio molecular orbital methods at the 6-31g level. Ab initio studies on the enantioselective catalytic reduction of aromatic ketone catalyzed by the CTO catalyst, however, have not been reported yet. In Parts 1 and 2 of this study [13, 14], the CTO catalyst **1**, the adduct **2**, the adduct **3**, and their properties were studied by means of the Hartree–Fock ab initio molecular orbital method at 6-31g* basis sets. The aim of this work is to investigate the structures of the CTO–alkoxyborane adduct **4** and its properties.

Computations and Results

For all the investigated systems, standard ab initio molecular orbital calculations were carried out. In Parts 1 and 2 of our study [13, 14], we indicated that the CTO–borane–ketone adduct **3** has four different structures and that borane coordinates at the N(3) site of the CTO catalyst **1**. [For the coordination of borane at the S(7) site, when the carbonyl oxygen of aromatic ketone coordinates at the B(2) site, the CTO–borane–ketone adduct is decomposed into aromatic ketone and the CTO–borane adduct after being optimized completely.] Also, the CTO–alkoxyborane adduct **4** has four structures, which are illustrated in Scheme 1. (Nevalainen substituted $HOBH_2$ and a simplified molecular model for the alkoxyborane $PhMeCHOBH_2$ and the CBS catalyst **1a**, respectively. Thus the conformations of the CBS–alkoxyborane adduct were not taken into account in his computations [11, 12].) All the structures of the CTO–alkoxyborane adduct **4** are optimized completely by means of the Hartree–Fock method at 6-31g* basis sets with program Gaussian 92. The optimized structures are shown in Figure 1. For all the structures, total energies, formation energies, dipole moments, and selected bond lengths are summarized in Table I. Mulliken overlap populations, which are given in parentheses, are also summarized in Table I. Selected atomic charges are shown in Table II. For the purpose of convenient discussion, selected bond

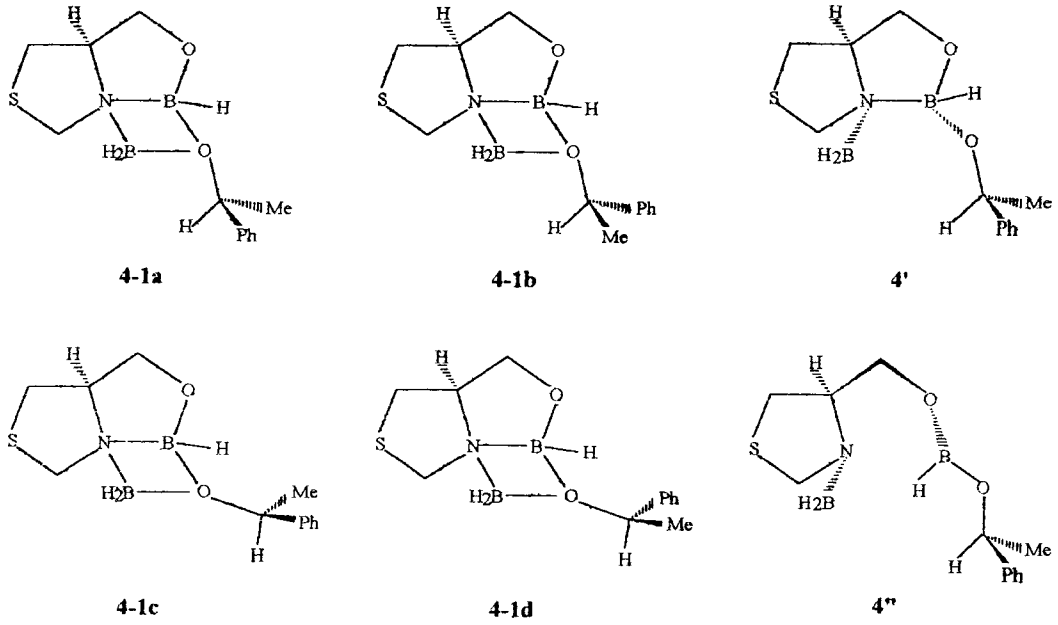

SCHEME 1.

lengths and Mulliken overlap populations for all the structures of the CTO–borane–ketone adduct **3** [14] are listed in Table III and selected atomic charges for **3** are presented in Table II, where **3-1a** corresponds to **4-1a** (i.e., the hydride transfer from the borane moiety to the carbonyl carbon of aromatic ketone **3-1a** leads to the structure **4-1a**), **3-1b** corresponds to **4-1b**, **3-1c** corresponds to **4-1c**, and **3-1d** corresponds to **4-1d**. In this article, to study chemical bonds in detail, a natural bond orbital (NBO) analysis for the CTO–alkoxyborane adduct is also carried out. Selected stabilization interaction energies $E(2)$ obtained from the second-order perturbative theory [15, 16] are listed in Table IV.

Discussion

The complete optimization of the investigated systems reveals that the CTO–alkoxyborane adduct **4** exists in four stable structures. They are in one-to-one correspondence with the four structures of the CTO–borane–ketone adduct **3** [14] and each of them contains a B-O-B-N four-membered ring. The optimized structures are illustrated in Figure 1. For the four optimized structures, the B_{BH2}–N(3)–B(2), N(3)–B(2)–O_{CO}, and B(2)–O_{CO}–B_{BH2} angles are **4-1a**, 87.80, 89.66, and 91.75°; **4-1b**, 87.79, 89.33, and 91.72°; **4-1c**, 87.54, 89.56, and 91.29°; **4-1d**, 88.64, 88.20, and 93.53°. B(2), N(3), B_{BH2}, and O_{CO} are located on the almost same plane. The O_{CO}–B(2)–N(3)–C(4) and B_{BH2}–N(3)–B(2)–O(1) torsion angles are **4-1a**, 123.15 and 108.06°; **4-1b**, 123.76 and 107.31°; **4-1c**, 113.71 and 115.87°; **4-1d**, 116.02 and 113.72°. The C_{CO}–O_{CO}–B(2) angles and the C_{CO}–O_{CO}–B(2)–N(3) torsion angles are **4-1a**, 125.15 and 41.53°; **4-1b**, 124.45 and 142.92°; **4-1c**, 124.69 and 135.94°; **4-1d**, 135.89 and 161.15°. As presented in Table I, the total energies of the optimized structures are **4-1a**, −1116.6421 au; **4-1b**, −1116.6410 au; **4-1c**, −1116.6420 au; **4-1d**, −1116.6406 au. Their corresponding formation energies are −160.34, −168.53, −171.42, and −147.05 kJ/mol. The formation reaction is exothermic. In addition, the energy difference between the structure **4-1d** with the highest energy and the structure **4-1a** with the lowest energy is only about 4 kJ/mol, which implies that the four structures of the CTO–alkoxyborane adduct **4** have about the same stability.

As shown in Table II, the negative charge of O(1) and the positive charges of B(2) and S(7) in the CTO–alkoxyborane adduct are almost equal to those in the CTO–borane–ketone adduct, whereas there is a low increase in the negative charge of N(3) in the CTO–alkoxyborane adduct. However, the charges of the carbonyl oxygen and the carbonyl carbon of aromatic ketone and the charge of B_{BH2} are changed considerably. The charges of O_{CO} and B_{BH2} for all the structures of the CTO–alkoxyborane

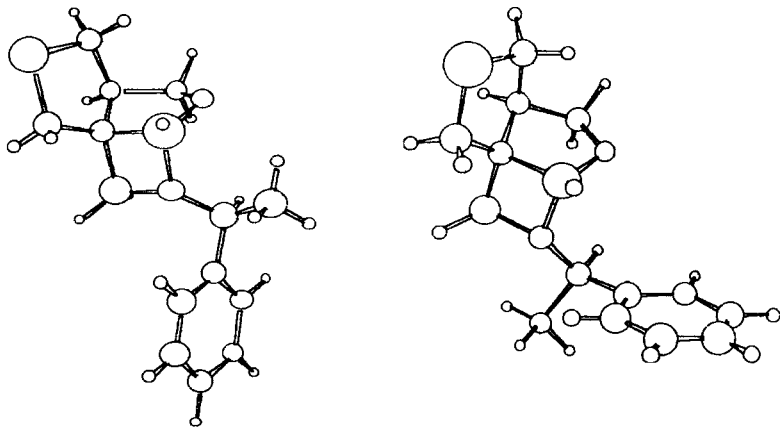

4-1a

4-1b

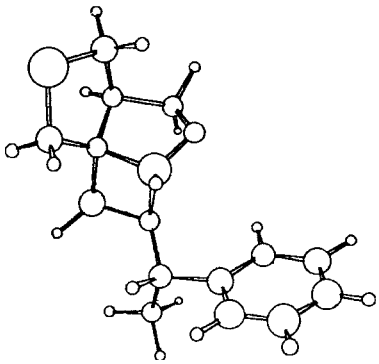

4-1c

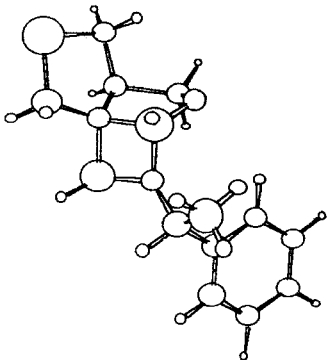

4-1d

FIGURE 1. The optimized structures of the CTO–alkoxyborane adduct.

TABLE I

Dipole moments *D* (D), total energies *E* (au), formation energies ΔE (kJ/mol), selected bond lengths (Å), and selected Mulliken overlap populations (in parentheses) for the CTO–alkoxyborane adduct.

	4-1a	4-1b	4-1c	4-1d
D	2.25	2.11	1.47	1.90
E	−1116.6421	−1116.6410	−1116.6420	−1116.6406
ΔE	−160.34	−168.53	−171.42	−147.05
C_{CO}—O_{CO}	1.426	1.426	1.427	1.422
	(0.145)	(0.147)	(0.144)	(0.148)
C_{CO}—Ph	1.515	1.515	1.515	1.516
	(0.351)	(0.361)	(0.357)	(0.340)
N(3)—B_{BH2}	1.613	1.607	1.600	1.610
	(0.203)	(0.211)	(0.209)	(0.207)
B(2)—N(3)	1.610	1.618	1.623	1.619
	(0.238)	(0.232)	(0.236)	(0.239)
O_{CO}—B(2)	1.567	1.568	1.571	1.563
	(0.135)	(0.132)	(0.122)	(0.129)
O_{CO}—B_{BH2}	1.548	1.546	1.547	1.533
	(0.188)	(0.193)	(0.189)	(0.195)

TABLE II

Selected atomic charges for the CTO–alkoxyborane adduct; those for the CTO–borane–ketone adduct are given in parentheses.

	4-1a (3-1a)	4-1b (3-1b)	4-1c (3-1c)	4-1d (3-1d)
O(1)	−0.722	−0.714	−0.698	−0.710
	(−0.720)	(−0.716)	(−0.698)	(−0.704)
N(3)	−0.807	−0.807	−0.814	−0.810
	(−0.772)	(−0.761)	(−0.732)	(−0.728)
O_{CO}	−0.802	−0.798	−0.821	−0.815
	(−0.628)	(−0.630)	(−0.625)	(−0.646)
B(2)	0.947	0.936	0.927	0.942
	(0.934)	(0.925)	(0.913)	(0.923)
S(7)	0.134	0.134	0.133	0.133
	(0.115)	(0.116)	(0.131)	(0.128)
C_{CO}	0.178	0.173	0.193	0.178
	(0.643)	(0.618)	(0.598)	(0.631)
B_{BH2}	0.478	0.486	0.492	0.491
	(0.167)	(0.158)	(0.152)	(0.142)

adduct, respectively, are **4-1a**, −802 and 0.478; **4-1b**, −0.798 and 0.486; **4-1c**, −0.821 and 0.492; **4-1d**, −0.815 and 0.491, which are much greater than those for all the structures of the CTO–borane–ketone adduct (**3-1a**, −0.628 and 0.167; **3-1b**, −0.630 and 0.158; **3-1c**, −0.625 and 0.152; **3-1d**, −0.646 and 0.142). Because of the great increase in the negative charges of O_{CO}, the interaction between O_{CO} and B_{BH2} is strengthened greatly and that between O_{CO} and B(2) is also strengthened. The positive charges of C_{CO} for all the structures of the CTO–alkoxyborane adduct (**4-1a**, 0.178; **4-1b**, 0.173; **4-1c**, 0.193; **4.1d**, 0.178) are decreased considerably in comparison with those for the four structures of the CTO–borane–ketone adduct (**3-1a**, 0.643; **3-1b**, 0.618; **3-1c**, 0.598; **3-1d**, 0.631). The reason for the decrease in the positive charges of C_{CO} is that a hydride transfers from the borane moiety to the carbonyl carbon of the aromatic ketone. The changes in atomic charges are in close relationship with molecular structures. As illustrated in Table I, in the four structures of the CTO–alkoxyborane adduct, the C_{CO}—O_{CO} and C_{CO}—Ph bond lengths are **4-1a**, 1.426 and 1.515 Å; **4-1b**, 1.426 and 1.515 Å; **4-1c**, 1.427 and 1.515 Å; **4-1d**, 1.422 and 1.516 Å. The corresponding Mulliken overlap populations are 0.145 and 0.351, 0.147 and 0.361, 0.144 and 0.357, and 0.148 and 0.340. By comparing the bond lengths and the Mulliken overlap populations for the four structures of the CTO–borane–ketone adduct illustrated in Table III, it is clear that the C_{CO}—O_{CO} and C_{CO}—Ph bond lengths for the four structures of the CTO–alkoxyborane adduct are increased greatly and the corresponding Mulliken overlap populations are decreased. In this case, the π bond in the carbonyl of aromatic ketone and the π bond between the carbonyl carbon and the phenyl are broken down and the C—O and C—Ph bonds are transformed into single σ bonds. Furthermore, since the interactions between O_{CO} and B_{BH2} and between O_{CO} and B(2) are strengthened greatly, the O_{CO}–B_{BH2} and O_{CO}–B(2) distances are decreased considerably to 1.5–1.6 Å and the corresponding Mulliken overlap populations are increased to 0.13–0.19. The considerable decrease in the O_{CO}–

TABLE III

Total energies *E* (au), selected bond lengths (Å), and selected Mulliken overlap populations for the CTO–borane–ketone adduct.

	3-1a	3-1b	3-1c	3-1d
E	1116.5810	1116.5768	−1116.5767	−1116.5846
C=O	1.227	1.223	1.216	1.223
	(0.418)	(0.442)	(0.470)	(0.449)
C_{CO}—Ph	1.477	1.476	1.480	1.479
	(0.410)	(0.385)	(0.370)	(0.409)
N(3)—B_{BH3}	1.664	1.676	1.660	1.654
	(0.173)	(0.166)	(0.173)	(0.176)
B(2)—N(3)	1.596	1.586	1.558	1.572
	(0.225)	(0.253)	(0.260)	(0.255)
O_{CO}—B(2)	1.581	1.633	1.734	1.644
	(0.129)	(0.092)	(0.058)	(0.081)
O_{CO}—B_{BH3}	2.843	2.830	3.016	3.007

TABLE IV
Selected stabilization interaction energies *E*(2) (kcal/mol) for the CTO–alkoxyborane adduct.

	Donor NBO		Acceptor NBO		*E*(2)
4-1a	LP(p)	O_{CO}	LP*(p)	B(2)	113.22
	LP(sp)	O_{CO}	LP*(p)	B(2)	157.43
	LP(p)	O_{CO}	Lp*(p)	B_{BH2}	57.39
	LP(sp)	O_{CO}	Lp*(p)	B_{BH2}	183.02
	BD(σ)	N(3)—B(2)	LP*(p)	B_{BH2}	230.94
	LP(p)	N(3)	LP*(p)	B_{BH2}	96.77
	LP(p)	N(3)	BD*(σ)	N(3)—B(2)	73.61
	LP(sp)	O_{CO}	BD*(σ)	N(3)—B(2)	18.98
4-1b	Lp(p)	O_{CO}	LP*(p)	B(2)	118.94
	LP(sp)	O_{CO}	LP*(p)	B(2)	152.54
	LP(p)	O_{CO}	LP*(p)	B_{BH2}	55.12
	LP(sp)	O_{CO}	LP*(p)	B_{BH2}	196.74
	BD(σ)	N(3)—B(2)	LP*(p)	B_{BH2}	250.74
	LP(p)	N(3)	LP*(p)	B_{BH2}	89.73
	LP(p)	N(3)	BD*(σ)	N(3)—B(2)	80.66
	LP(sp)	O_{CO}	BD*(σ)	N(3)—B(2)	19.56
4-1c	LP(p)	O_{CO}	LP*(p)	B(2)	117.79
	LP(sp)	O_{CO}	LP*(p)	B(2)	156.72
	LP(p)	O_{CO}	LP*(p)	B_{BH2}	56.12
	LP(sp)	O_{CO}	LP*(p)	B_{BH2}	199.04
	BD(σ)	N(3)—B(2)	LP*(p)	B_{BH2}	260.90
	LP(p)	N(3)	LP*(p)	B_{BH2}	88.02
	LP(p)	N(3)	BD*(σ)	N(3)—B(2)	82.45
	LP(sp)	O_{CO}	BD*(σ)	N(3)—B(2)	20.31
4-1d	LP(p)	O_{CO}	LP*(p)	B(2)	125.73
	LP(sp)	O_{CO}	LP*(p)	B(2)	158.95
	LP(p)	O_{CO}	LP*(p)	B_{BH2}	53.79
	LP(sp)	O_{CO}	LP*(p)	B_{BH2}	189.08
	BD(σ)	N(3)—B(2)	LP*(p)	B_{BH2}	237.24
	LP(p)	N(3)	LP*(p)	B_{BH2}	93.97
	LP(p)	N(3)	BD*(σ)	N(3)—B(2)	79.44
	LP(sp)	O_{CO}	BD*(σ)	N(3)—B(2)	19.94

B_{BH2} and O_{CO}–B(2) distances ultimately leads to the formation of the B-O-B-N four-membered ring in the CTO–alkoxyborane adduct. The formation of the four-membered ring causes the N(3)—B_{BH2} bond to become shorter (about 1.61 Å) and the B(2)—N(3) bond to become longer (about 1.62 Å). Their overlap populations are changed correspondingly. The increase in the B(2)—N(3) bond may be caused by the tensile stress generated from the four-membered ring in the CTO–alkoxyborane adduct.

According to the mechanism of the enantioselective reduction of ketone catalyzed by the CBS catalyst proposed by Corey et al. [15], the hydride transfer of the adduct **3** to the adduct **4** passes through an intermediary state similar to **4′** in structure (see Scheme 1). From the ab initio molecular orbital results for the CBS enantioselective reduction, Nevalainen indicated that this intermediary state **4′** was unstable [7, 8]. Although we have made every effort to try to optimize the structure of **4′**, a optimized structure like **4′** has not been obtained. The optimization for **4′** leads to the optimized structure **4′′** shown in Scheme 1, not to the optimized intermediary state **4′**; i.e., the B(2)—N(3) bond in **4′** is broken down during the optimization. This result may imply either that the intermediary state **4′** is quite unstable (or no nexistent), or that the hydride transfer from the borane moiety to the carbonyl carbon of aromatic ketone in **3** occurs at the same time as the formation of the B-O-B-N four-membered ring in **4**. As indicated above,

while a hydride transfers from the borane moiety to the carbonyl carbon of aromatic ketone in **3**, the negative charge of the carbonyl oxygen of aromatic ketone and the positive charge of B_{BH3} are increased considerably, which causes the interaction between O_{CO} and B_{BH3} to be strengthened greatly. It can be anticipated from these results that with a hydride transfering toward the carbonyl carbon of aromatic ketone, the interaction between O_{CO} and B_{BH3} is strengthened by degrees; in other words, the distance between O_{CO} and B_{BH3} is shortened gradually with a hydride transfer. Based on this expectation and on the fact that the optimization for **4′** leads to the structure **4″**, it is reasonable that the hydride transfer from the borane moiety to the carbonyl carbon ot ketone occurs simultaneously with the formation of the B-O-B-N four-membered ring.

To analyze the structures of the CTO–alkoxyborane adduct in more detail, an NBO analysis was carried out. For all the structures of the CTO–alkoxyborane adduct, selected stabilization interaction energies $E(2)$ obtained from the second-order perturbative theory [15, 16] are summarized in Table IV, where BD and BD* represent bonding and antibonding natural bond orbitals, respectively, and LP and LP* are lone pairs and empty orbitals. In the natural bond orbital analysis, $E(2)$ is used to describe the interaction between the donor bond and the acceptor bond of an intramolecule or to describe the delocalization trend of electrons from a donor bond to an acceptor bond. As presented in Table IV, the stabilization interaction energies $E(2)$ between the lone pairs of O_{CO} and the empty p orbital of B(2) and those between the lone pairs of O_{CO} and the empty p orbital of B_{BH2} are approximately **4-1a**, 270 and 240 kcal/mol; **4-1b**, 271 and 252 kcal/mol; **4-1c**, 274 and 255 kcal/mol; **4-1d**, 285 and 243 kcal/mol. $E(2)$ between the lone pairs of N(3) and the empty p orbital of B_{BH2} plus those between the B(2)—N(3) bonding orbital and the empty p orbital of B_{BH2} are also considerable for all the structures of the CTO–alkoxyborane adduct. These results show that the tendencies for electron transfer from O_{CO} and N(3) toward the empty p orbitals of B_{BH2} and B(2) are quite strong; i.e., the coordination potentialities between O_{CO} and B(2), O_{CO} and B_{BH2}, and N(3) and B_{BH2} are great. In other words, there are the strong interactions between O_{CO} and B(2), O_{CO} and B_{BH2}, and N(3) and B_{BH2}. These strong interactions lead to the formation of the B-O-B-N four-membered ring in the CTO–alkoxyborane adduct **4**, although there is strong tensile stress in the four-membered ring. In addition, it is seen from Table IV that $E(2)$ between the B(2)—N(3) antibonding orbital and the lone pairs of N(3) and O_{CO} are considerable for all the structures of the CTO–alkoxyborane adduct, which implies that the potentiality of the electron acceptance of the B(2)—N(3) antibonding orbital is strong. This result also causes the B(2)—N(3) bond to be weakened greatly. Comparison of Table I with Table III shows that the B(2)—N(3) bond lengths are increased greatly. Therefore, the B(2)—N(3) bond may be broken down during the decomposition of the CTO–alkoxyborane adduct.

Conclusions

As shown in the above discussions, the chiral cyclic sulfur-containing oxazaborolidine **1** (the CTO catalyst) reacts with aromatic ketone in the presence of borane to form the catalyst–alkoxyborane adduct with a B-O-B-N four-membered ring. The B-O-B-N four-membered ring is stable, although there is strong tensile stress in the four-membered ring. The catalyst–alkoxyborane adduct exists in four stable structures. Among these structures, the largest energy difference is only about 4 kJ/mol. In the catalyst–alkoxyborane adduct, the B(2)—N(3) bond in the catalyst is weakened greatly, which may lead to its breakdown during the decomposition of the CTO–alkoxyborane adduct.

ACKNOWLEDGMENTS

This work was supported by the Science Foundation of National Education Department and the Science Foundation of Chongqing City, People's Republic of China.

References

1. Li, X. S.; Xie, R. G. Tetrahedron: Asymmetry 1996, 7, 2779.
2. Huang, H.-L.; Lin, Y.-C.; Chen, S.-F.; Wang, C.-L. J.; Liu, L.-T. Tetrahedron: Asymmetry 1996, 7, 3067.
3. Reiners, I.; Martens, J.; Schwarz, S.; Henkel, H. Tetrahedron: Asymmetry 1996, 7, 1763.
4. Trentmann, W.; Mehler, T.; Martens, J. Tetrahedron: Asymmetry 1997, 8, 2033.
5. Carey, E. J.; Bakshi, R. K.; Shibata, S. J Am Chem Soc 1987, 109, 5551.
6. Nevalainen, V. Tetrahedron: Asymmetry 1991, 2, 827.
7. Nevalainen, V. Tetrahedron: Asymmetry 1991, 2, 1133.
8. Nevalainen, V. Tetrahedron: Asymmetry 1992, 3, 1563.
9. Nevalainen, V. Tetrahedron: Asymmetry 1992, 3, 1441.

10. Nevalainen, V. Tetrahedron: Asymmetry 1993, 4, 1597.
11. Nevalainen, V. Tetrahedron: Asymmetry 1992, 3, 921.
12. Nevalainen, V. Tetrahedron: Asymmetry 1994, 5, 903.
13. Li, M.; Xie, R. G.; Hu, C. W.; Wang, X.; Tian, A. M. Int J Quantum Chemistry 2000, 78, 245–251.
14. Li, M.; Xie, R. G.; Tian, S. H.; Tian, A. M. Int J Quantum Chemistry 2000, 78, 252–260.
15. Reed, A. E.; Curtiss, L. A.; Weinhold, F. Chem Rev 1988, 88, 899.
16. Reed, A. E.; Weinstock, R. B.; Weinhold, F. J Chem Phys 1985, 83, 735.